Numerical study of the effect of laser-frequency fluctuations on optical bistability

Steven M. Moore*
Department of Physics and Astronomy, University of Massachusetts, Amherst, Massachusetts 01003
(Received 26 June 1985)

A numerical study of the effect of laser-frequency fluctuations on dispersive optical bistability shows a strong dependence on the strength and correlation time of the noise. Both the stationary-state characteristics and switching times are studied, and a qualitative explanation is provided for some of the numerical results.

I. INTRODUCTION

Absorptive optical bistability (AOB) was theoretically predicted by Szöke *et al.*[1] in 1969. Five years later, McCall[2] predicted the transistor effect and treated AOB in a Fabry-Perot cavity by a numerical analysis of the Maxwell-Bloch equations. This work was followed by the experiments of Gibbs, McCall, and Venkatesan in Na and ruby, in which both transistor operation and bistability were observed.[3,4] The analysis of their data showed that the observed bistability was mainly of dispersive type. This dispersive optical bistability (DOB) can be modeled by the equations[5]

$$\dot{x}=y\cos\phi-x-2cx/(a^2+x^2)\ , \tag{1.1a}$$

$$\dot{\phi}=-y(\sin\phi)/x+2c\Delta/(a^2+x^2)\ . \tag{1.1b}$$

Δ, the atomic detuning parameter, measures the dispersion; $\Delta=0$ corresponds to the purely absorptive case. y is the input amplitude from the laser, x is the response amplitude, ϕ is the phase difference, c is the bifurcation parameter, and $a^2=1+\Delta^2$. The usual dimensionless variables have been employed.[5-8]

Although Eqs. (1.1) have their origin in a semiclassical theory, we will call them the deterministic equations since our objective is to consider the effect of fluctuations. Many theoretical studies have been made on the effect of noise on the optically bistable system. Fluctuations in c have been studied on several occasions.[6-9] These consist of fluctuations in the optical pumping rate, the atomic density, and spontaneous emissions. All three are quite small unless one purposely increases the first two. The case of a weak, isotropic, additive noise has also been treated.[10] Noise produced by the driving laser has only recently begun to be considered. Here one must consider both the possibility of laser-amplitude and of laser-frequency (or phase) fluctuations. A theoretical study of the effect of laser-amplitude fluctuations for the absorptive case was made by Kuś *et al.*;[11] they found that the amplitude fluctuations have no practical importance.

Thus, our interest here is to study the effect of laser-frequency fluctuations on the behavior of the optically bistable system described by Eqs. (1.1). Our study is numerical because very little can be said analytically about the highly nonlinear problem posed by (1.1) in the presence of frequency fluctuations.

Previous numerical work along these lines was done by Cresser and Meystre.[12] They actually studied the effect of phase noise, which is related to frequency noise. Willis[13,14] has theoretically studied both frequency and phase fluctuations. Our numerical results together with their qualitative explanation are intended to complement those just mentioned. In their simulations Cresser and Meystre only studied the case of white noise for AOB and did not examine the steady states under fluctuations. Willis's calculations use the linear approximation.

Ignoring all other fluctuations and following Willis,[13] we arrive at the following system of stochastic differential equations (SDE's) describing the effect of laser-frequency fluctuations on the optically bistable system:

$$\dot{x}=y\cos\phi-x-2cx/(a^2+x^2)\ , \tag{1.2a}$$

$$\dot{\phi}=-y(\sin\phi)/x+2c\Delta/(a^2+x^2)+\epsilon\alpha\ . \tag{1.2b}$$

Here, $\Omega=\epsilon\alpha$ is the noise term with strength measured by ϵ. In our study, α will either be normalized white noise (zero mean and correlation equal to a delta function) or Ornstein-Uhlenbeck noise [zero mean and correlation equal to $\exp(-|t-t'|/\tau)/2\tau$], the latter modeling the effect of a positive correlation time τ. α as white noise was the case considered by Cresser and Meystre[12] (their linewidth parameter corresponds to our $\epsilon^2/2$) and corresponds to the common assumption[15] that the phase of the laser is driven by white noise. Willis,[13] however, considers correlation times as large as 10^4 in the dimensionless time units used here.

The organization of this paper is as follows. In Sec. II, we will make some comments on the deterministic system (1.1), mostly to see what the orders of magnitude of the relaxation times are. In Sec. III the main results of the numerical study are given, and a qualitative explanation of them is presented in Sec. IV. Appendix A describes the simulation algorithm. In Appendix B two of the basic equations of Sec. IV are derived.

II. COMMENTS ON THE DETERMINISTIC EQUATIONS

Graham and Schenzle[10] made a general stability analysis of the deterministic equations (1.1). Changing to rectangular coordinates (X and Y denote the components of the response field, and the input field E_0 is taken in the X direction), they showed that one has global stability outside the circle of radius $E_0/2$ and center $(E_0/2,0)$. Therefore, since the equations are first order and autonomous, the only attractors within this circle can be fixed

points and limit cycles.

A simple theorem[16] shows that no periodic orbits can exist: Given an autonomous system $\dot{X}=F(X,Y)$, $\dot{Y}=G(X,Y)$, let F and G have continuous first-order partial derivatives in a simply connected domain D. If F_X+G_Y has the same sign throughout D, then there is no periodic solution lying entirely in D.

For the case at hand, F_X+G_Y is negative everywhere. Thus, for all practical purposes, the only attractors for the system (1.1) are the deterministic stationary states defined by $\dot{x}=0$, $\dot{\phi}=0$ (we now return to using polar coordinates). For these one has the state equation[5]

$$y=x\{[1+2c/(a^2+x^2)]+[2c\Delta/(a^2+x^2)]^2\}^{1/2}, \tag{2.1}$$

giving y as a function of x, or x as a multivalued function of y, and

$$\tan\phi=2c\Delta/(a^2+x^2+2c) \tag{2.2}$$

determining ϕ implicitly as a multivalued function of y (i.e., both x and ϕ exhibit bistability). We call the state corresponding to small x the opaque state and the state corresponding to large x the transparent state. These have $dy/dx>0$ and are stable. The stationary states where $dy/dx<0$ are unstable.[5]

It is useful to have some estimates on the times for relaxation to the stationary states. For small deviations δx and $\delta\phi$ from these states, one has the linear relation

$$\begin{bmatrix}\delta\dot{x}\\ \delta\dot{\phi}\end{bmatrix}=\begin{bmatrix}A & B\\ C & D\end{bmatrix}\begin{bmatrix}\delta x\\ \delta\phi\end{bmatrix}, \tag{2.3}$$

determined by the matrix elements

$$A=-1-2c/(a^2+x^2)+4cx^2/(a^2+x^2)^2, \tag{2.4a}$$

$$B=-2c\Delta x/(a^2+x^2), \tag{2.4b}$$

$$C=2c\Delta/x(a^2+x^2)-4c\Delta x/(a^2+x^2)^2, \tag{2.4c}$$

$$D=-1-2c/(a^2+x^2). \tag{2.4d}$$

The real parts of the characteristic values λ of the matrix in (2.3) must be negative in order to have linear stability. Figure 1 is a graph of $-\mathrm{Re}\lambda$ versus y for the stable stationary states, for $c=20$ and $\Delta=3$, the values of c and Δ which will be used in the following discussion.

For small x, each λ has an imaginary part, hence the relaxation to the opaque state is oscillatory. Moreover, this state is characterized by fairly large $-\mathrm{Re}\lambda(\sim 5)$, i.e., the relaxation is fast. On the other hand, for very large x, $\lambda\sim -1$, so one has nonoscillatory relaxation to the transparent state. Hence, the relaxation is relatively slow.

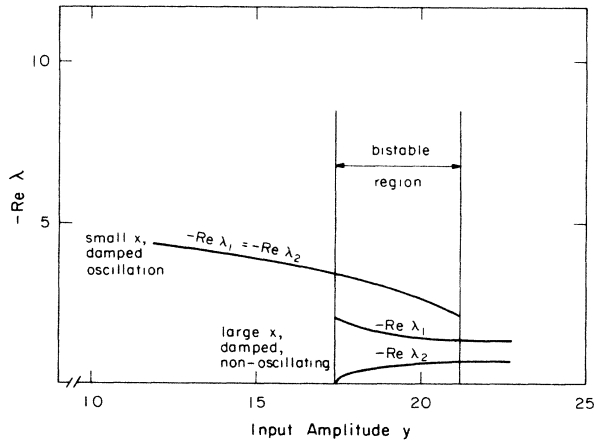

FIG. 1. The negative of the real part of the characteristic value, $-\mathrm{Re}\lambda$, vs input amplitude y for $C=20$, $\Delta=3$.

III. NUMERICAL STUDY

A variation of the algorithm used by Sancho *et al.*[17] was employed in order to study the system (1.2) numerically. This algorithm and some features of the computer program are described in Appendix A.

For Figs. 2–5 and Table I, a noise strength of $\epsilon=1$ was

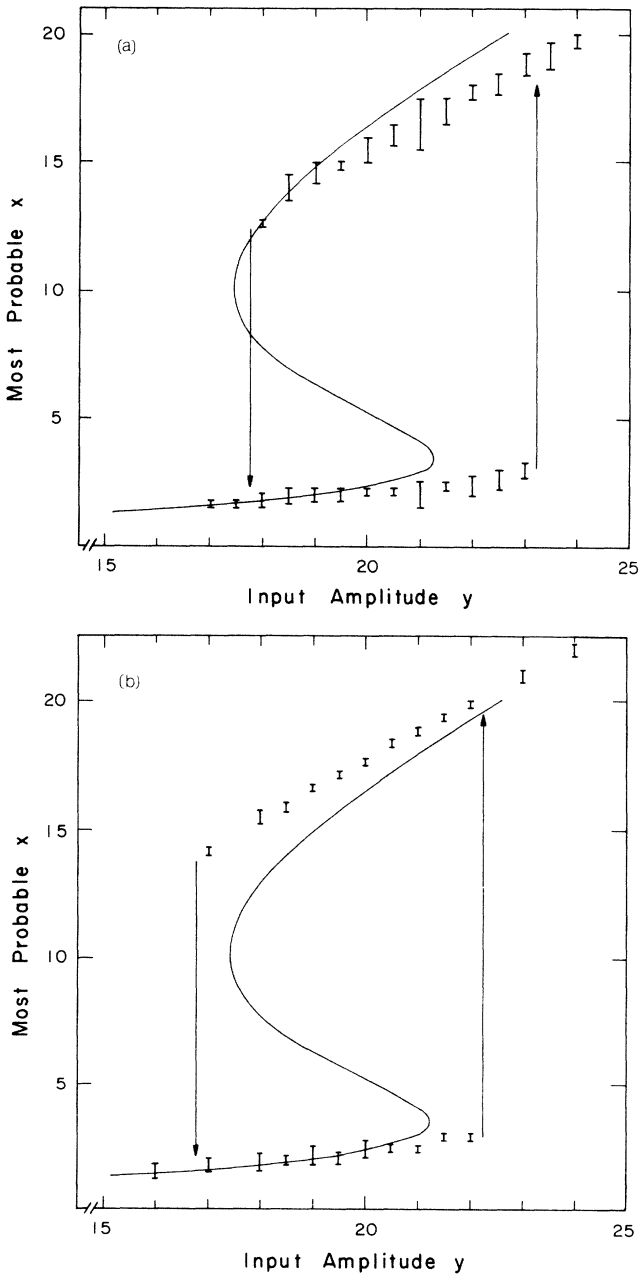

FIG. 2. (a) Most probable x vs input amplitude y for $\epsilon=1$, $\tau=0$. (b) Most probable x vs input amplitude y for $\epsilon=1$, $\tau=5$.

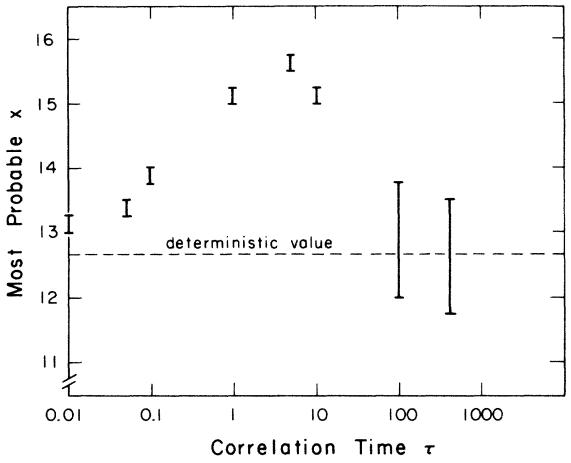

FIG. 3. Most probable x vs correlation time τ for input amplitude $y=18$.

used. Values of ϵ between 10^{-2} and 10 are physically plausible. We chose $\epsilon=1$ for pedagogical reasons (it allows the effect of the noise to be easily seen) and to permit the effects of noise to be observed in relatively short computer runs.

Figure 2(a) shows the most probable x (i.e., the local

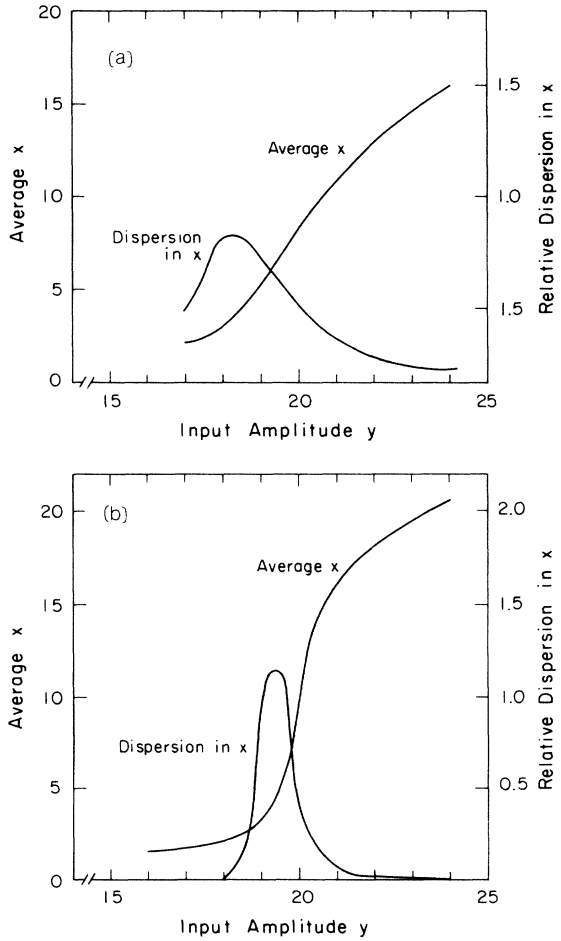

FIG. 4. (a) Average x and relative dispersion in x vs input amplitude y for $\epsilon=1$, $\tau=0$. (b) Average x and relative dispersion in x vs input amplitude y for $\epsilon=1$, $\tau=5$.

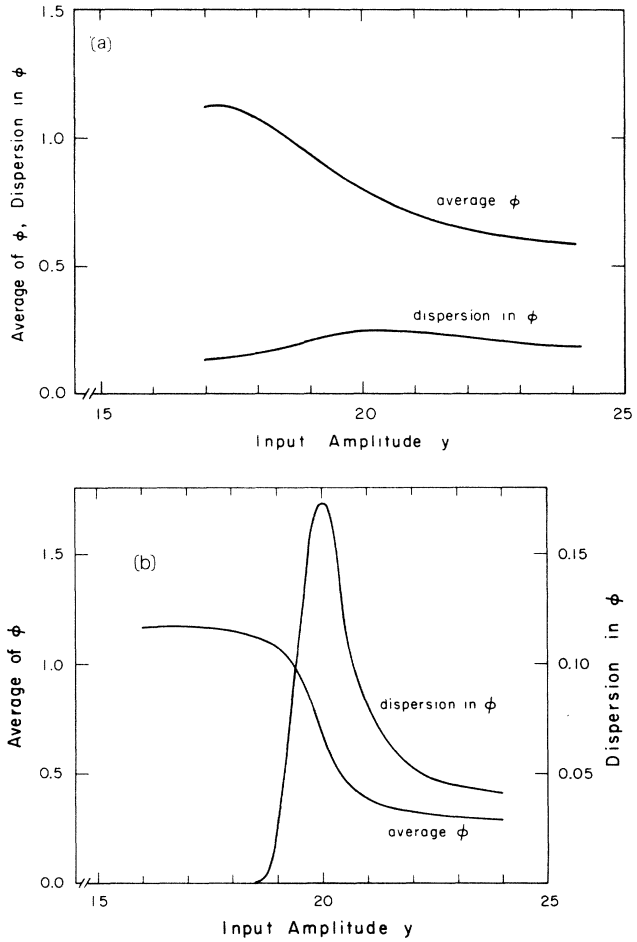

FIG. 5. (a) Average ϕ and dispersion in ϕ vs input amplitude y for $\epsilon=1$, $\tau=0$. (b) Average ϕ and dispersion ϕ vs amplitude y for $\epsilon=1$, $\tau=5$.

maxima of the probability distribution) as a function of the input amplitude y for white noise ($\tau=0$). Also shown is the deterministic curve (solid line) for comparison. The arrows indicate that the state disappears beyond that value of y (the computer obviously cannot follow the unstable deterministic states). Figure 2(b) shows the most probable x as a function of y for $\tau=5$. A general feature to note in these figures is that for white noise, for the

TABLE I. Switching times as a function of input amplitude y.

y	Forward $\tau=0$	Forward $\tau=5$	Backward $\tau=0$	Backward $\tau=5$
18.0	125.1	>500	8.6	34.2
18.5	106.9	>500	10.7	46.1
19.0	36.1	>500	17.1	66.0
19.5	66.9	273.1	13.1	115.7
20.0	27.6	116.4	22.1	151.1
20.5	23.0	56.6	30.8	272.7
21.0	20.0	38.1	38.3	367.8
21.5	15.6	27.0	45.7	>500
22.0	15.8	27.3	45.5	>500
22.5	15.5	24.4	49.4	>500
23.0	13.8	21.1	66.6	>500

TABLE II. Switching times as a function of ϵ for $\tau=0$ and $y=19$.

ϵ	Forward	Backward
1.00	66.9	13.1
0.95	68.3	13.2
0.90	72.5	13.7
0.85	76.4	15.3
0.80	91.3	15.3
0.75	101.9	17.7
0.70	115.3	20.1
0.65	146.5	24.1
0.60	165.1	25.1
0.55	255.0	36.3

same small x the presence of noise produces a larger y (extension of the lower part of the curve). This is certainly less pronounced for Ornstein-Uhlenbeck noise, where the small-x portion of the curve disappears for some y between 22 and 23. This behavior in τ is qualitatively different than what happens for fluctuations in the bifurcation parameter.[9]

Figure 3 exhibits the most probable x as a function of τ for $y=18$. Note that a maximum occurs around $\tau=5$, which is why $\tau=5$ was chosen for the positive τ runs corresponding to Fig. 2(b).

Figures 4(a) and 4(b) show the average x and the relative dispersion of x versus y for $\tau=0$ and 5. Note the peaking of the relative dispersion in the center of the bistable region, a feature already noted in absorptive OB for fluctuations in the bifurcation parameter.[6] The peak value for white noise corresponds to a y somewhere between 18 and 19, tending towards 18, which is why we chose $y=18$ to examine the explicit dependence on τ.

Figures 5(a) and 5(b) show the average relative phase ϕ and the dispersion of ϕ versus y for $\tau=0$ and 5. Note the different scales for the dispersion. In both cases the peaking of the dispersion in ϕ occurs at a different y value than the one for the peaking of the relative dispersion in x.

Table I shows the switching times, both forward and backward, and still $\epsilon=1$. By forward switching time we mean how long it takes to switch from a region around the most probable x and ϕ corresponding to the opaque state to a region around the most probable x and ϕ corresponding to the transparent state. The backward switching time corresponds to a transition in the opposite sense. The entries >500 in the table only indicate that no switching took place before stopping the integration routine on the computer, which ran in all cases to $t=500$.

It is also useful to study the dependence of the switching time on ϵ. Table II shows this for white noise and ϵ decreasing from $\epsilon=1$, all for $y=19$.

IV. QUALITATIVE EXPLANATION OF THE NUMERICAL RESULTS

In this section, we will give a qualitative explanation of some of the numerical results. The general picture developed from examining the computer runs is one where x and ϕ fluctuate close to one deterministic stationary state for some time and then move rapidly to a region close to the other deterministic state where there are again small amplitude fluctuations until the next switching event. This suggests a general approximation for determining the two most probable values corresponding to these deterministic states, namely to ignore the presence of the other state. All of the qualitative analysis that follows depends on this idea.

One consequence of our general approximation philosophy is that in the following we will be cavalier about the distinction between average values within the well and most probable values. This is permitted as long as we consider only those fluctuations which are close to the deterministic values of x, excluding all considerations of the other ones. Such a procedure makes sense as long as the switching times are much longer than the deterministic relaxation times, which is the case here.

From an examination of Figs. 2 and 3, one sees that there are essentially four regimes. First of all, there is the white-noise limit $\tau\rightarrow 0$. This unfortunately does not fit on Fig. 3, but Fig. 2(b) shows that it corresponds to a slight negative displacement from the deterministic point at $y=18$. Then there is a regime corresponding to a small, positive value of τ (say, $0<\tau\leq 0.01$), where there is a definite displacement above the deterministic curve. There is a third regime for moderate values of τ ($0.01\leq\tau\leq 300$), and finally a fourth regime for very large values of τ ($\tau>300$). We give a qualitative explanation of regimes 1, 2, and 4.

For the first regime, let us obtain an estimate of the size of the fluctuations using the linear approximation. We have from Eq. (2.3) with noise the following expressions for the correlations (see Appendix B):

$$\langle\delta x^2\rangle=\int d\omega\, B^2 G(\omega)\,, \tag{4.1a}$$

$$\langle\delta\phi^2\rangle=\int d\omega (A^2+\omega^2) G(\omega)\,, \tag{4.1b}$$

$$\langle\delta x\delta\phi\rangle=-\int d\omega\, ABG(\omega)\,, \tag{4.1c}$$

with

$$G(\omega)=S(\omega)/[(\omega^2-AD+BC)^2+(A+D)^2\omega^2]\,. \tag{4.2}$$

The coefficients A,B,C,D are given in Eqs. (2.4); $S(\omega)$ is the spectral density of the noise. At $y=18$ and for the transparent state (large x) we find that white noise gives $\langle\delta x^2\rangle^{1/2}/x\sim 0.7\epsilon$, $\langle\delta\phi^2\rangle^{1/2}\sim 1.2\epsilon$. For the opaque state (small x) we find that $\langle\delta x^2\rangle^{1/2}/x\sim 0.6\epsilon$, $\langle\delta\phi^2\rangle^{1/2}\sim 1.2\epsilon$.

Let us now examine a perturbation series in ϵ. All the correlations (4.1) are of order ϵ^2 because of the presence of this term in $S(\omega)$, while $\langle\delta x\rangle$ and $\langle\delta\phi\rangle$ are zero only to order ϵ. Thus one can expand to quadratic terms in $\delta x,\delta\phi$, and use (4.1) to obtain $\langle\delta x\rangle$ and $\langle\delta\phi\rangle$ to order ϵ^2. We are interested in $\langle\delta x\rangle$, and the result is (see Appendix B)

$$\langle\delta x\rangle=(AD-BC)^{-1}\times\int d\omega\, G(\omega)[(B\alpha_2-D\alpha_1)B^2-(B\beta_2-D\beta_1)AB+(B\gamma_2-D\gamma_1)(A^2+\omega^2)]\,, \tag{4.3}$$

where

$$\alpha_1=6cx/(a^2+x^2)^2-8cx^3/(a^2+x^2)^3 , \tag{4.4a}$$

$$\alpha_2=-y(\sin\phi)/x^3-2c\Delta/(a^2+x^2) +8c\Delta x^2/(a^2+x^2)^3 , \tag{4.4b}$$

$$\beta_1=0 , \tag{4.4c}$$

$$\beta_2=y(\cos\phi)/x^2 , \tag{4.4d}$$

$$\gamma_1=-y(\cos\phi)/2 , \tag{4.4e}$$

$$\gamma_2=y(\sin\phi)/2x . \tag{4.4f}$$

Let us denote the expression in square brackets in (4.3) by $g+h\omega^2$. This polynomial together with $AD-BC$ determine the sign of $\langle\delta x\rangle$.

We find that $g>0$ and $h<0$ for $x\leq 3.6$. In this same range of x, $AD-BC>0$. For increasing ω, g is soon dominated by $h\omega^2$, so we have that $\langle\delta x\rangle<0$. Thus the behavior for Fig. 2 for $y\sim 21$, $x\sim 2$ is now qualitatively understood: $\langle\delta x\rangle<0$ means a downward displacement of the curve. This downward displacement is less for small but positive τ, because of the presence of τ in $S(\omega)$.

For large x and white noise, a similar reasoning explains the behavior of the most probable x curve. We find that both coefficients g and h are negative for $x\geq 3.8$. Moreover, $AD-BC$ is positive for $x\geq 10.2$. Thus $\langle\delta x\rangle<0$ in the range $x\geq 10.2$. Thus the white-noise behavior at $y\sim 21$, $x\sim 15.5$ is qualitatively understood: $\langle\delta x\rangle<0$ means a downward displacement of the curve, but this displacement is less in magnitude for larger τ.

In both cases we see the tendency to move up for increasing τ. However, for large x this quadratic approximation is obviously not the whole story because $\langle\delta x\rangle$ becomes positive for large enough τ.

For the other extreme case where τ is very large, Eqs. (1.2) can be treated as if $\Omega=\epsilon\alpha$ were a constant. One obtains the state equation

$$y^2=x^2\{[1+2c/(a^2+x^2)]^2+[\Omega+2c\Delta/(a^2+x^2)]^2\} . \tag{4.5}$$

Although Fig. 3 is for fixed y, it is actually easier to consider (4.5) for fixed x because of the bistable behavior of x as a function of y. In this case,

$$y(\Omega,x)\simeq y(0,x)+\left.\frac{\partial y}{\partial x}\right|_{\Omega=0}\Omega+\frac{1}{2}\left.\frac{\partial^2 y}{\partial x^2}\right|_{\Omega=0}\Omega^2 , \tag{4.6}$$

so

$$\langle\delta y\rangle\simeq\frac{1}{4\tau}\left.\frac{\partial^2 y}{\partial\Omega^2}\right|_{\Omega=0} . \tag{4.7}$$

Since

$$\left.\frac{\partial^2 y}{\partial\Omega^2}\right|_{\Omega=0}=x\left[\frac{x}{y}-\frac{1}{4}\left[\frac{x}{y}\right]^3[4c\Delta/(a^2+x^2)]^2\right] , \tag{4.8}$$

$\langle\delta y\rangle$ is positive for $x\sim 12.7$. A positive displacement in y for the same x is equivalent to a negative displacement in x for the same y. Note that (4.7) shows that this correction becomes vanishingly small as τ increases. Hence we have an explanation of the behavior of Fig. 3 for very large τ, which for $\tau=300$ is not inconsistent with a small negative displacement $\langle\delta x\rangle$. Unfortunately the behavior in the intermediate region, where τ is close to the deterministic relaxation times, is more difficult to explain. This is because the laser-frequency fluctuation is mathematically equivalent to a fluctuating cavity detuning [compare Eq. (4.5) to Agrawal and Carmichael's Eq. (3.12), Ref. 5], and the bistability is notoriously sensitive to cavity detuning (see Fig. 2 of Agrawal and Carmichael).

Nevertheless, the following argument offers a qualitative explanation of Fig. 3's positive displacement in x with respect to the deterministic curve for small τ, and has the advantage of taking more of the nonlinearities into account (nonlinearities must be an important factor here because the most probable x for $0.01\leq\tau\leq 0.1$ are well separated from the deterministic values). Let us expand (1.2a) around the most probable ϕ, call it $\tilde{\phi}$. Then we have

$$\dot{x}\simeq y\cos\tilde{\phi}-y(\sin\tilde{\phi})\delta\phi-x-2cx/(a^2+x^2) \tag{4.9}$$

to first order in $\delta\phi$, the deviation of ϕ from $\tilde{\phi}$. For the transparent state, $\tilde{\phi}$ is small (from the simulations, $\tilde{\phi}\sim 0.1$), so for all practical purposes x only sees second-order corrections to $\tilde{\phi}$. That means that an approximation to the state equation is

$$y=[x+2cx/(1+x^2)]/\cos\tilde{\phi} , \tag{4.10}$$

which is obtained by ignoring the $\delta\phi$ term in (4.9) and setting $\dot{x}=0$.

$\tilde{\phi}$ is determined by treating x as a parameter in (1.2b) and solving the corresponding one-dimensional approximate Fokker-Planck equation.[9] Note that this assumes that both ϵ and τ are small. Treating x as a parameter has some justification in the fact that Eqs. (4.1) show that $\langle\delta x^2\rangle$ gets smaller with increasing τ, whereas $\langle\delta\phi^2\rangle$ stays about the same. We find

$$\tilde{\phi}\simeq\tan^{-1}[2c\Delta/(a^2+x^2+2c)(1+\tau\epsilon^2/2)] . \tag{4.11}$$

Comparing with (2.1) and (2.2), we see that for the same x, $\tilde{\phi}$ is smaller than the deterministic ϕ, thus giving a smaller y. This is equivalent to saying that for the same y, x is larger.

This qualitatively explains the behavior seen in Fig. 3 where $\langle\delta x\rangle$ becomes positive for $\tau=0.1$. Note that this analysis cannot be made for the opaque state because in (4.9) $\tilde{\phi}\sim 1.1$, so $\sin\tilde{\phi}\sim 0.9$. Also note that the phenomenon we are trying to explain (positive $\langle\delta x\rangle$ for the transparent state) has nothing to do with bistability; Fig. 2(b) shows that it occurs outside the bistable zone as well. The larger x is, the better the approximation we have used becomes, since $\tilde{\phi}$ gets smaller for larger x. Although Eq. (4.11) shows that the correction to first order in τ is x independent, Fig. 2(b) actually shows the correction increasing with decreasing x. This can be attributed to a second-order effect in τ which is a function of x.

This last approximation procedure has been successful in giving a qualitative explanation for the location of the most probable x for small τ, but one should be wary of using it to predict a more global property like the switching times. Moreover, we note that there is some indica-

tion that the approximate Fokker-Planck equation used here (and in Ref. 17) may have problems with global descriptions even without making the additional approximation we made.[18] Since this two-dimensional problem of estimating switching times depends on a good estimate of the stationary probability density, we will make no attempts in this direction.

However, the general trend for the switching times is clear and offers no surprises. At the turning points, the switching times are the same order of magnitude of the delays reported experimentally[19] and predicted theoretically for AOB without considering fluctuations.[20] The fluctuations keep the delay from becoming arbitrarily large. In Table I we see that switching times for $\tau=5$ are greater than those for $\tau=0$. One intuitive reason for this, of course, is that larger frequencies are absent, i.e., the noise does not fluctuate as fast. However, there is another reason: the distance between the transparent and opaque states is larger for $\tau=5$ than for $\tau=0$. For Table II we note that the forward or backward switching time T_s seems to be well described by the functional relation

$$T_s = T_0 \exp(\epsilon_0^2/\epsilon^2) . \tag{4.12}$$

The constant T_0, of course, depends on whether forward or backward switching times are considered ($T_0 \sim 35$ for forward, 8 for backward). The Arrhenius factor ϵ_0^2 is the same for both and is approximately 0.25. This type of behavior is what one would expect if the problem were of one dimension. In that case the probability density varies as $\exp(-U/\epsilon^2)$ where U is some potential function. The switching times would then have the behavior of (4.12) according to the usual activation analysis. In fact, a two-dimensional analysis using the same generic isotropic diffusion of Graham and Schenzle[10] was made by Talkner and Hanggi;[21] they found for the special case of cavity detuning equal to atomic detuning relaxation times of the same general form as (4.12), in spite of the fact that our diffusion term is not isotropic.

It should be observed that we have both phase up-switching and down-switching in this system as opposed to what Cresser and Meystre have observed for the absorptive case.[12] Thus it is difficult to compare the behavior indicated by (4.12) and its associated parameters with their results, especially since the $\Delta=3$ deterministic curve is very different than the $\Delta=0$ deterministic curve (although our value of $y=19$ plays a similar role as their value of $y=15$—both are in the middle of the deterministic bistable region).

Nevertheless, the switching times of Table II are qualitatively similar to those of Cresser and Meystre for the absorptive case. They are surprisingly small for a moderate bandwidth, although they rapidly decrease with bandwidth if (4.12) holds true. Only a bandwidth as small as that corresponding to $\epsilon=0.1$ would result in very large switching times.

V. CONCLUSIONS AND FINAL REMARKS

A general conclusion to be obtained from our numerical study is that the effects of laser-frequency fluctuations (i.e., the finite linewidth of the laser) are far from being negligible. In fact it is very important to consider them when one wishes to use the optically bistable device as a switching element. We now outline some of these practical considerations.

The analysis of the location of the opaque and transparent states has shown that, with a slow decrease in input amplitude with white noise in the fluctuating frequency, the switch from upper to lower bistable branch would tend to occur on the average at input field strengths higher than those for the perfectly coherent situation. On the other hand, the existence of a positive correlation time dramatically changes this behavior; for a correlation time on the order of the deterministic relaxation times, one expects that the switch from upper to lower bistable branch would tend to occur at input field strengths lower than those for the perfectly coherent situation.

The switching-time behavior is also interesting. For the case where the laser linewidth is of the same order as the cavity bandwidth, the smallness of the switching times implies that the optically bistable device has little use as a switching device. In fact, it is clear from our analysis that a small correlation time and large linewidth do away with bistability in the sense that the spontaneous switching will occur on a microscopic time scale. However, we have also shown that these switching times strongly depend on the correlation time and the linewidth in a way that increasing the first and decreasing the second are practical methods for increasing the switching times.

ACKNOWLEDGMENTS

The author wishes to thank S. Cohen, A. DeFonzo, R. Guyer, and J. Machta for useful discussions.

APPENDIX A

The simulation algorithm employed in the numerical study of Eqs. (1.2) is a slight variation of the one of Sancho *et al.*[17]

In the case that α is Orstein-Uhlenbeck noise we write (1.2) in the form

$$\dot{x} = f_1(x,\phi) , \tag{A1a}$$

$$\dot{\phi} = f_2(x,\phi) + \epsilon\alpha , \tag{A1b}$$

$$\dot{\alpha} = -\alpha/\tau + \alpha_w/\tau , \tag{A1c}$$

where α_w is normalized white noise (having a delta-function correlation). This means that α is a normalized Ornstein-Uhlenbeck noise [having correlation equal to $\exp(-|t-t'|/\tau)/2\tau$].

The algorithm corresponding to Eqs. (A1) is (Δ is the step size here, not the atomic detuning parameter)

$$x(t+\Delta) = x(t) + \mathscr{A}(\mathrm{RK}_1) + \frac{\epsilon}{2}\Delta^2 \frac{\partial f_1(x(t),\phi(t))}{\partial\phi}\alpha(t) , \tag{A2a}$$

$$\phi(t+\Delta) = \phi(t) + \mathscr{A}(\mathrm{RK}_2) + \frac{\epsilon}{2}\Delta^2 \frac{\partial f_2(x(t),\phi(t))}{\partial\phi}\alpha(t) + \epsilon[\Delta\alpha(t) - \Delta^2\alpha(t)/2\tau + X_2(t)] , \tag{A2b}$$

$$\alpha(t+\Delta) = \alpha(t) - \Delta\alpha(t)/\tau + X_1(t)/\tau . \tag{A2c}$$

Here

$$X_1(t)=\Delta^{1/2}\gamma_1(t)\ ,$$

$$X_2(t)=\frac{1}{\sqrt{2}}\Delta^{3/2}\left[\frac{1}{\sqrt{2}}\gamma_1(t)+\frac{1}{\sqrt{6}}\gamma_2(t)\right]\ ,$$

and γ_1 and γ_2 are independent Gaussian random numbers with zero mean and variance 1. $\mathscr{A}(\mathrm{RK}_1)$ and $\mathscr{A}(\mathrm{RK}_2)$ are simple Runge-Kutta approximations in the deterministic sense (these are used to guarantee good deterministic trajectories when the noise is small).

When $\tau\to 0$, $\Delta\alpha\sim X_1$, so one obtains the following algorithm, valid to order Δ:

$$x(t+\Delta)=x(t)+\mathscr{A}(\mathrm{RK}_1)\ , \tag{A3a}$$

$$\phi(t+\Delta)=\phi(t)+\mathscr{A}(\mathrm{RK}_2)+\epsilon X_1(t)\ . \tag{A3b}$$

This was used to simulate the effect of white noise.

We tested the noise simulation in various ways. For approximately 4000 iterations, for example, the simulated variances for $\tau=1$ and 10 were never more than 2% different than the desired variances, and the magnitude of the averages were less than 10^{-2}. A fast Fourier transform of the time series generated in this test showed that the required $1/\omega^2$ behavior of the spectrum was obtained for $\omega\sim 1/\tau$. This latter test was insensitive to low frequencies, but since it showed an essentially flat spectrum for white noise, we can be fairly certain that the spectral characteristics of the noise are correct.

In the numerical study described in Sec. IV a step size of $\Delta=0.05$ was used, except for $\tau=0.01$ and 0.05 where $\Delta=0.001$ was used. Time averaging and ensemble averaging were employed together in developing the state statistics (Figs. 2–5); this consisted of recording the trajectory values at every 20 integration steps, starting at $t=10$ and going to $t=500$, and then averaging over the 50 Monte Carlo runs. The most probable x and other values were determined from a histogram having $\Delta x=0.25$, $\Delta\phi=2\pi/80$. The widths in the bars in Figs. 2 and 3 correspond to multiples of Δx. Widths of multiple values of Δx are due to cases where the peaks were very flat. These are effective error bars, then, due to the histogram grid size and the inherent limitations of a finite statistical sample.

There is a some error involved in using a dynamical simulation to determine the stationary probability distribution (i.e., one assumes the ergodic limit is already achieved). This was tested in a few cases by letting the program run somewhat longer than $t=500$ (limitations in computer time prohibited an order-of-magnitude increase). No differences were noted in the most probable x values within the histogram grid size described above. Sensitivity to initial conditions was also tested (see below).

Obviously the switching times correspond only to ensemble averaging. These were determined by examining a region around the deterministic states (the same Δx and $\Delta\phi$ were used), starting the trajectory in one of them, and recording when the trajectory entered each grid square around the other. After finishing the 50 runs, one has an average entry time to each grid square. After determining the most probable x and ϕ, one examines the region around them and selects the earliest time. Here the half-maximum rule was used to determine the region studied around the most probable values.

Note that because both forward and backward switching times are determined, one actually has a test as to whether the steady-state statistics depend on initial conditions (which is really a test of whether one has reached the ergodic limit, since presumably in that limit the steady state *is* independent of initial conditions). Within the accuracy of the unorthodox error bars defined above, no difference was detected between starting the system in the opaque or transparent states. Also, the values of x, ϕ, and the dispersions of these variables (which are independent of the histogram grid size chosen), were seen to be independent of this choice of initial state.

There is considerable noise in the switching times due to the finite sample size used (50 Monte Carlo runs) as well as the finite Δx and $\Delta\phi$. For these reasons, the data are presented in tabular form just as they came out of the program and no attempt of establishing traditional error bars was made. The data are interesting in spite of these limitations because they agree with general intuitive expectations (see Sec. IV) even in this complicated two-dimensional, nonlinear and nonisotropic noise problem. It is believed that more statistical precision (extending to 500 Monte Carlo runs, for example) will not change the general trends.

It should be pointed out that, due to the nature of the simulation program, "switching" as used here refers to an essentially different process than that studied recently be Erneux and Mandel.[22] They consider the behavior when y is varied in time. Their study is also deterministic in that no fluctuations are included. In the analysis made in this paper, the system has a fixed y value and the switching is driven solely by the laser-frequency fluctuations. It is worthwhile to observe that a generalization of the Erneux-Mandel analysis to include fluctuations is a difficult problem, although it certainly could be studied using the numerical methods discussed here.

APPENDIX B

In this appendix we derive Eqs. (4.1)—(4.4). Let us write the stochastic differential equations in the form

$$\dot{x}=f_1(x,\phi)\ , \tag{B1a}$$

$$\dot{\phi}=f_2(x,\phi)+\Omega\ , \tag{B1b}$$

where

$$f_1(x,\phi)=y\cos\phi-x-\frac{2cx}{a^2+x^2}\ , \tag{B2a}$$

$$f_2(x,\phi)=-\frac{y}{x}\sin\phi+\frac{2c\Delta}{a^2+x^2}\ . \tag{B2b}$$

Then the linearized equations are obtained by writing $x=\bar{x}+\delta x$, $\phi=\bar{\phi}+\delta\phi$, where $\bar{x}$ and $\bar{\phi}$ are the deterministic values (deterministic opaque or transparent state), and expanding f_1 and f_2 to first order. Let

$$M=\begin{bmatrix}A & B\\ C & D\end{bmatrix}\ , \tag{B3}$$

$$N=\begin{bmatrix}0\\ \Omega\end{bmatrix} \tag{B4}$$

(recall that $\Omega=\epsilon\alpha$, where α is normalized white noise or Ornstein-Uhlenbeck noise). The linearized equations then read

$$\dot{z}=Mz+N\ , \tag{B5}$$

where z is the column vector $\binom{\delta x}{\delta\phi}$. Taking Fourier transforms, one finds

$$z(\omega)=(-M+i\omega)^{-1}N(\omega)\ . \tag{B6}$$

Rewriting this in terms of the components and taking the inverse of the matrix, one has

$$\delta x(\omega)=B\Omega(\omega)/[-BC+(-D+i\omega)(-A+i\omega)]\ , \tag{B7a}$$

$$\delta\phi(\omega)=(-A+i\omega)\Omega(\omega)/[-BC+(-D+i\omega)(-A+i\omega)]\ . \tag{B7b}$$

Since $\langle\Omega(\omega)\Omega^*(\omega')\rangle=S(\omega)\delta(\omega-\omega')$, $S(\omega)$ being the spectral density of the noise, one finally obtains Eqs. (4.1).

For the quadratic analysis one expands f_1 and f_2 to second order in δx and $\delta\phi$. In the same shorthand notation as above, one can write the resulting system of stochastic differential equations as

$$\dot{z}=Mz+G(z)+N\ , \tag{B8}$$

where G is a vector function of the vector z with components

$$G_x=\alpha_1\delta x^2+\beta_1\delta x\,\delta\phi+\gamma_1\delta\phi^2\ , \tag{B9a}$$

$$G_\phi=\alpha_2\delta x^2+\beta_2\delta x\,\delta\phi+\gamma_2\delta\phi^2\ . \tag{B9b}$$

α_1, β_1, etc., are related to the partial derivatives of f_1 and f_2 and are given in the main text (appropriate factors of 2 have been included). From (B8), one sees that

$$\langle z\rangle=-M^{-1}\langle G(z)\rangle\ . \tag{B10}$$

In other words,

$$\langle\delta x\rangle=-\langle DG_x-BG_\phi\rangle/(AD-BC)\ , \tag{B11}$$

which just gives Eq. (4.3).

*Present address: Department of Physics, Rensselaer Polytechnic Institute, Troy, NY 12181.

[1]A. Szöke, V. Danen, J. Goldhar, and N. A. Kurnit, Appl. Phys. Lett. **15**, 376 (1969).
[2]S. L. McCall, Phys. Rev. A **9**, 1515 (1974).
[3]H. M. Gibbs, S. L. McCall, and T. N. C. Venkateson, Phys. Rev. Lett. **36**, 113 (1976).
[4]T. N. C. Venkateson and S. L. McCall, Appl. Phys. Lett. **30**, 282 (1977).
[5]G. P. Agrawal and H. J. Carmichael, Phys. Rev. A **19**, 2074 (1979).
[6]R. Bonifacio, M. Gronchi, and L. A. Lugiato, Phys. Rev. A **18**, 2266 (1978).
[7]A. R. Bulsara, W. C. Schieve, and R. F. Gragg, Phys. Lett. **68A**, 294 (1978).
[8]J. C. Englund, W. C. Schieve, W. Zurek, and R. F. Gragg, in *Optical Bistability,* edited by C. M. Bowden, M. Cifton, and H. R. Robl (Plenum, New York, 1981), pp. 315–335.
[9]S. M. Moore, Nuovo Cimento **79B**, 125 (1984).
[10]R. Graham and A. Schenzle, Phys. Rev. A **23**, 1302 (1981).
[11]M. Kuś, K. Wodkiewicz, and J. A. C. Gallas, Phys. Rev. A **28**, 214 (1983).
[12]J. Cresser and P. Meystre, in Ref. 8, pp. 265–280.
[13]C. R. Willis, Phys. Rev. A **27**, 375 (1983).
[14]C. R. Willis, Phys. Rev. A **29**, 774 (1984).
[15]M. Sargent III, M. O. Scully, and W. E. Lamb, Jr., *Laser Physics* (Addison-Wesley, Reading, Mass., 1974).
[16]W. E. Boyce and R. C. Diprima, *Elementary Differential Equations and Boundary Value Problems,* 3rd ed. (Wiley, New York, 1977).
[17]J. M. Sancho, M. San Miguel, S. J. Katz, and J. D. Gunton, Phys. Rev. A **26**, 1589 (1982).
[18]P. Hanggi, F. Marchesoni, and P. Grigolini, Z. Phys. B **56**, 333 (1984); P. Hanggi, T. J. Mroczkowski, F. Moss, and P. V. E. McClintock, Phys. Rev. A **32**, 695 (1985).
[19]D. E. Grant and H. J. Kimble, Opt. Commun. **44**, 415 (1983).
[20]R. Bonifacio and P. Meystre, Opt. Commun. **29**, 131 (1979).
[21]P. Talkner and P. Hanggi, Phys. Rev. A **29**, 768 (1984).
[22]T. Erneux and P. Mandel, Phys. Rev. A **28**, 896 (1983).